Report: **Scientific achievements in 2019**
Project: **1059**
Project title: **H2020 Blue-Action: Arctic Impact on Weather and Climate**
Coordinator: **Dr. Daniela Matei**
PIs: Dr. Daniela Matei, Dr. Jürgen Bader, Dr. Johann Jungclaus, Dr. Katja Lohmann, Dr. Elisa Manzini
Allocated period: **2019-01-01 to 2019-12-31**

Arctic warming impacts by atmospheric pathway

What drives the Warm Arctic Cold Eurasia (WACE) pattern in the winter (DJF) surface air temperature (SAT) trend is one of the most debated research topics in the last decade. Extensive analysis of observations and climate models output have led to opposing conclusions about the role of the Arctic sea ice (SIC) in driving the recent cooling trend over Eurasia. The observed studies suggest a key role for the Arctic SIC (e.g., Mori et al. 2014), whereas research with climate models claims it to be due to the internal atmospheric variability (e.g., McCusker et al. 2016). Here, we use the Blue-Action coordinated experiments and ERA-interim reanalysis to investigate if there is any fundamental underlying dynamical difference between the model response to the Arctic SIC and observations. For this purpose, we first identify a region confined over the Barents Sea (74N-80N, 20E-68E), that has seen the highest winter Arctic SIC loss in the last decades (Fig. 1a). The SAT over this region has a close association with the regional SIC changes (Mori et al. 2014). Hence, we use the SAT over the Barents Sea as a proxy index for understanding the associated sea ice response over the Northern Hemisphere (NH) SAT, in reanalysis and model outputs. We first focus in our analysis on reanalysis and the 10-member ensemble of AGCM sensitivity experiments performed with ECHAM6.3-HR, and then extend our investigation to the Blue-Action large ensemble. We construct the Barents Sea SAT index for each ensemble members of EXP1 (AMIP) and EXP2 (AMIP-sicCLIM), to evaluate the associated SAT response in the model experiments with and without observed SIC variations over the Arctic (Fig 1c, d).

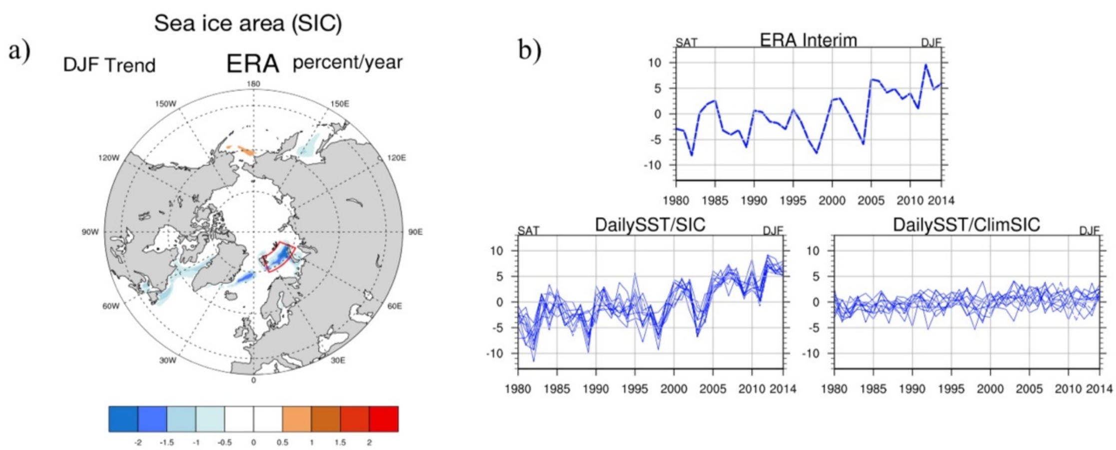

Fig. 1 a) The winter (DJF) mean sea ice area (SIC) trend in percent/year over the Northern Hemisphere in ERA-Interim reanalysis for the period 1980 to 2013. b) The time series of area averaged 2-meter air temperature (SAT) anomaly over the red box in figure a), which is showing the highest negative trend in the Barents Sea for the period 1980 to 2013 (top), the same time series of SAT anomalies but for the 10 ensemble members of the ECHAM6.3 in EXP1 (bottom left) and for the EXP2 (bottom right). All units for the SAT anomalies are in Kelvin (K). (from Ghosh et al., 2019)

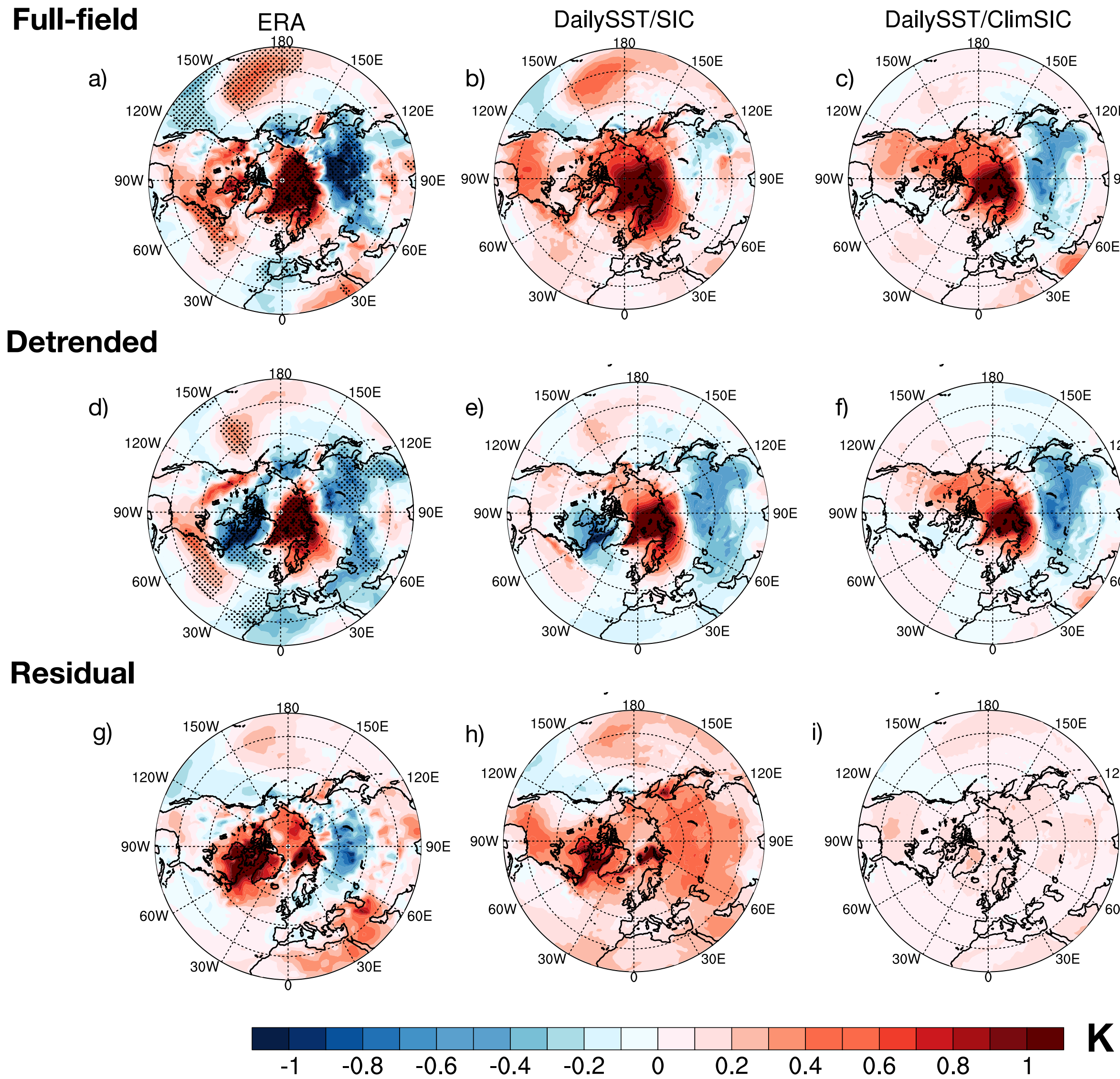

Fig. 1 a) *The NH SAT change for 1 standard deviation change in the Barents Sea SAT index shown in figure 1.a).* ***b)*** *the same as in a) but the ensemble mean of respective NH SAT changes for the 10 ensemble members of the EXP1 in ECHAM6.3.* ***c)*** *the same as in b) but for the EXP2 with daily climatological SIC over the Arctic.* ***d)****The NH detrended SAT change for 1 standard deviation change in the detrended Barents Sea SAT index.* ***e)*** *the same as in d) but the ensemble mean of the NH detrended SAT changes for the 10 ensemble members of the EXP1 in ECHAM6.3.* ***f)*** *the same as in e) but for the EXP2 with daily climatological SIC over the Arctic.* ***g)*** *The residual or difference of the figure a) from the figure c).* ***h)*** *The same residual or difference but for the figure b) and the figure e).* ***i)*** *The residual or difference but for the figure c) and figure f). All units are in Kelvin. Stippling in figure a) and c) represents the regions significant at p> 0.05. (from Ghosh et al., 2019)*

The full-field regression of the SAT on the Barents Sea SAT index in the reanalysis resembles the WACE pattern (Fig 2a). The warmer Arctic condition is centered over the Barents-Kara Sea region, while the colder Eurasia is centered on the central-to-eastern Eurasia. The full field regression of EXP1 (with daily varying SST and SIC) does not show a similarly strong cooling pattern over Eurasia in association with the warming over Arctic (Fig 2b), whereas in the EXP2 (Fig 2c, with the daily climatological SIC), we find a clearly prominent WACE, similar to reanalysis. This finding implies that the observed WACE pattern also exists in the model, though under the forcing of observed daily SIC variations, this WACE association weakens in the model. The regression analysis using the detrended (quadratic) field of SAT on the detrended Barents Sea SAT index reveals in reanalysis a similarly warm anomaly of the WACE pattern over the Arctic as seen with the full-field (Fig 2d). However, the center of the negative anomalies over Eurasia shifts eastward. Interestingly, the regression analysis of the detrended fields for the EXP1 reveals a prominent WACE pattern (Fig 2e). In association to a warm Arctic, it shows negative anomalies encompassing central to eastern Eurasia. This finding indicates that the WACE pattern also exists in the EXP1 under the forcing of observed SIC variations. Therefore, it is the trend related part of the variations that weakens in the model experiments. Consistently with the experimental design, the changes over Eurasia from full-field to detrended are much more striking for the EXP1 than for the EXP2 (Fig 2b,c,e,f). Indeed, the presence of WACE in EXP2 shows that the WACE is not dependent on either the inter-annual variation or the trend of the Arctic SIC, suggesting that it is a feature of atmospheric internal variability, possibly associated with Ural blocking. However, the detrended field EXP1 also shows a WACE (Fig 2e), indicating that the observed interannual SIC variation might have an association with the Eurasian SAT. There is therefore a possibility for the coupling of the WACE internal mode of variability with the interannually varying Barents SIC forced SAT.

The residual of the full-field regression still shows a cooling over Eurasia (albeit of smaller amplitude) in the reanalysis (Fig 2g). In the EXP1 and EXP2, the residual or the trend pattern does not bring any cold anomalies over Eurasia (Fig 2h,i). Instead both the experiments show warm anomalies throughout the Eurasian continent. The warm anomalies are larger in magnitude in EXP1 than in EXP2, as it can be expected due to the Arctic warming trend. In EXP2, the warm anomalies mainly depict the effect of radiative forcing and SST trends. In EXP1, there is an additional warming from the long-term trend of SIC. The question is therefore, why are the observed and simulated SAT trends different over Eurasia? To answer this question, we perform an EOF analysis of the SAT over Eurasia to compare the nature of variations of SAT in the model with the observations (Fig 3).

The first mode of SAT variability in the reanalysis shows a continent wide warming pattern, which has its center over middle Eurasia, the location of the observed cooling trend (Fig 3a, Fig 2g). This mode of variations could be related to the Arctic Oscillation (Mori et al. 2014). The second mode of variability is the WACE mode, which has its Warm center over the Barents Kara Sea and Cold center over the central to eastern Eurasia (Fig 3b). Interestingly, the region of cooling trend in the reanalysis is influenced by both modes, and hence the trend over this region is determined by the combination of the evolution of both modes. However, PC1 in the reanalysis does not yet show any long-term trend (black line in Fig 3c), but its negative phase at the end of the analyzed time period may play a major role in enhancing the cooling trend. Therefore, a part of the observed cooling is influenced by the internal variability of the PC1 that does not show any long-term trend and also no association with the Barents SIC variations. The long-term changes in the SIC gets associated with the PC2, which shows a positive trend with correlation of 0.91 with the SIC variations (black line Fig 3d), which means it is bringing more cooling over the central-to-eastern Eurasia with the warming Arctic. Compared to the reanalysis, the model simulated PC1 shows a clear positive trend in EXP1 (blue lines in Fig 3c). A positive trend in the first mode of SAT variations, whose positive phase leads to a continent-wide warming, would naturally lead to an overall warming trend. The second mode of variations also shows an upward trend (blue lines in Fig 3d). By extending the analysis to the other project models, and in doing so extending the ensemble size to 145 members, we find a general positive trend in both PC1 and PC2 for

EXP1 (Fig 3e). The trends in the PC1 and PC2 seems to be anticorrelated. The observed trend (black dot in Fig 3e) lies at the side of a significant positive trend in PC2 with no significant trend in PC1 (though not significant, a negative trend is present in the observed PC1 due to the intense negative phase at the end of the time period). The trend of the PCs in the EXP2 reveals the role of SIC in driving a positive trend in PC2. Without SIC forcing (EXP2), there is no negative PC2 trend emerging from the ensemble, while PC1 mostly shows positive trends, though very few are significant (Fig 3f). However, it seems SIC forcing also affect the trend in the PC1, given its slight increase (compare Fig 3e and 3f).

In summary, out results suggest that there is an overall positive trend in the first mode of SAT variations over Eurasia in the models, which is not observed in the last 35 years. This causes the models to not simulate the WACE trend pattern, which occurs due to the positive trend in the second mode of variability, combined with no trend in the first mode of variability (Ghosh et.al., in prep).

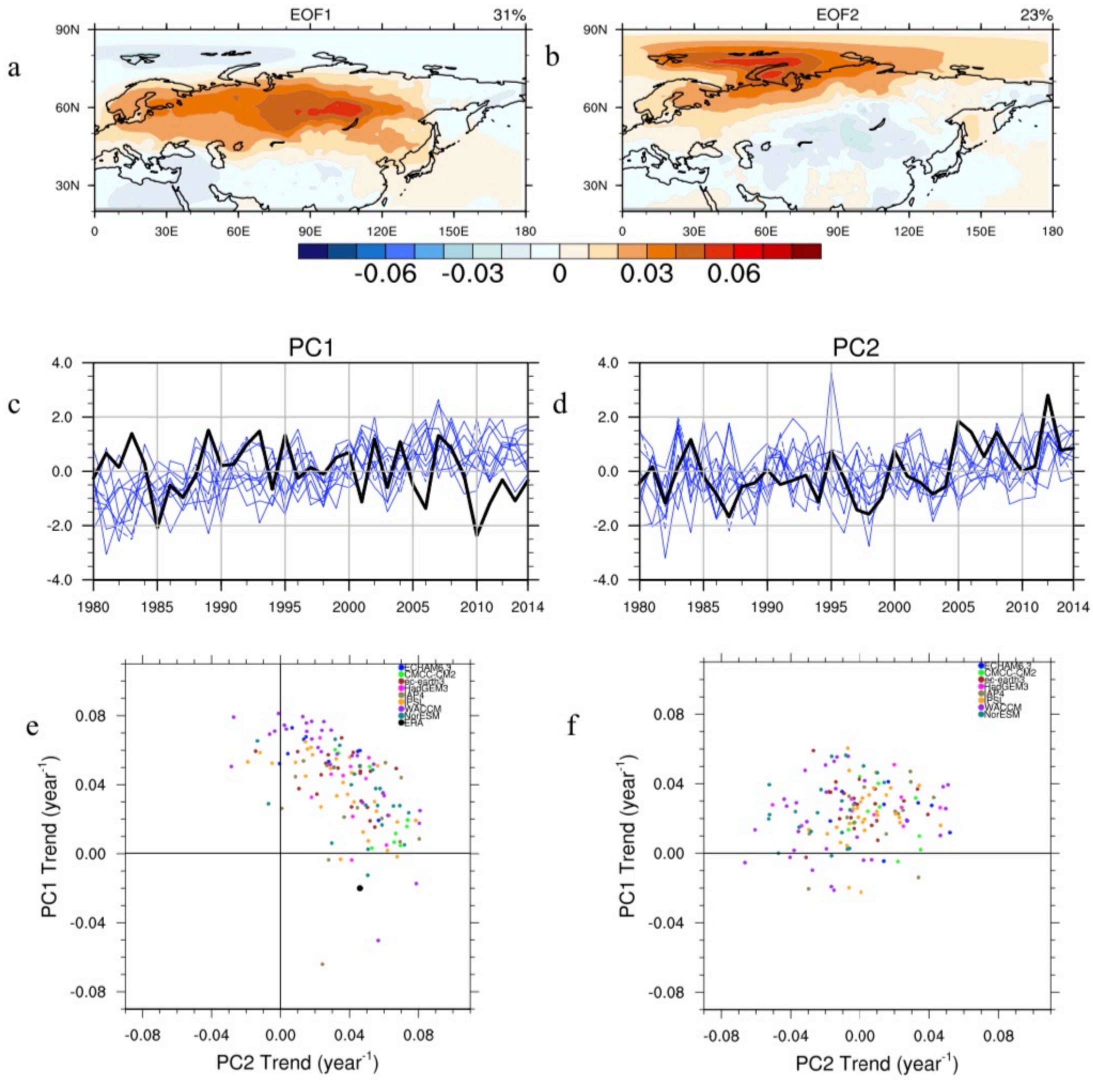

Fig. 3 a) The EOF1 and b) EOF2 patterns of the winter SAT in the ERA-Interim reanalysis over the Eurasian region (20-90N, 0-180E) for the observed period of 1980 to 2014. c) The associated normalized PC1 (in black) and the blue time series are also the same but for the 10 ensemble members of the EXP1 with observed daily SIC and SST boundary forcing. d) the same as in a) but for the PC2. e) Scatter plot of the normalized PC1 and PC2 trends of Eurasian SAT (in year-1) in EXP1 for the 8 models participated in coordinated experiments (in colored dots) and in the ERA (black dot) and f) the same as in c) but for the EXP2 with climatological daily SST/SIC forcing. (from Ghosh et al., 2019)

1. Ghosh R., D. Matei, E. Manzini, J. Bader, E. Tyrlis, A. Cherchi, J. Mecking, G. Gastineau, Y-C Liang, L. Suo, T. Tian, Y. Zhang, S. Yang, C. Frankignoul, Y. Gao, 2019: Warm Arctic Cold Eurasia in winter surface air temperature: driven by Barents Sea Ice loss or internal atmospheric variability? (in preparation)
2. Mori, M., Watanabe, M., Shiogama, H., Inoue, J. & Kimoto, M. Robust Arctic sea-ice influence on the frequent Eurasian cold winters in past decades (Nature Geoscience (2014) 7 (869-873)). *Nat. Geosci.* **8**, 159 (2015).
3. Sun, L., Perlwitz, J. & Hoerling, M. What caused the recent "Warm Arctic, Cold Continents" trend pattern in winter temperatures? *Geophys. Res. Lett.* **43**, 5345–5352 (2016).
4. Ogawa, F. *et al.* Evaluating Impacts of Recent Arctic Sea Ice Loss on the Northern Hemisphere Winter Climate Change. *Geophys. Res. Lett.* **45**, 3255–3263 (2018).
5. McCusker, K. E., Fyfe, J. C. & Sigmond, M. Twenty-five winters of unexpected Eurasian cooling unlikely due to Arctic sea-ice loss. *Nat. Geosci.* **9**, 838–842 (2016).